August 27-31, 2023
FLORENCE - ITALY
ICWE 16
16th International Conference on Wind Engineering

Validating multiphase numerical simulation of shoaling waves impacting a cylinder

Max Beeman[1], Hanul Hwang[2], Catherine Gorlé[3]

[1]*Stanford University, Stanford, CA, USA, mbeeman@stanford.edu*
[2] *Stanford University, Stanford, CA, USA, hanul@stanford.edu*
[3] *Stanford University, Stanford, CA, USA, gorle@stanford.edu*

SUMMARY:
During a hurricane, buildings are exposed to many different factors that cause damage, including storm surge flooding, subsequent wave loading, and exposure to high winds. The long-term aim of this work is to quantify sources of uncertainty in a numerical framework capable of representing the full multiphase physics of hurricane loading on structures. In the current work, numerical simulation results representing a subset of the full physics, namely waves impacting a structure with no mean wind, will be validated against an experimental dataset. In addition, an initial analysis of the effect of the waves on the air phase will be performed. The open-source computational fluid dynamics framework OpenFOAM is used for large-eddy simulations with wave generation through IHFOAM and the isoAdvector interface capturing scheme. The accuracy of these modelling tools in matching wave propagation and structural loading from experimental results is examined, as are the impacts of modelling choices on air phase results.

Keywords: Wind-Wave Interaction, Computational Fluid Dynamics (CFD), Large Eddy Simulation (LES)

1. INTRODUCTION

During a hurricane, buildings are exposed to many different sources of damage, including storm surge flooding, subsequent wave loading, and exposure to high winds. One common method to mitigate storm surge damage is to build structures elevated above expected flood levels, known as stilt houses. However, this design exposes the home to an elevated, higher wind speed portion of the wind profile, and introduces an aerodynamic gap above wavy flood waters beneath the home that could alter the probability of wind damage in ways that are not yet understood.

The long-term aim of this work is to validate a numerical framework capable of representing the complex multiphysics of hurricane loading, in order to aid evaluation and design of severe weather adaptation measures. Numerical simulation results will be validated against experimental datasets representing subsets of the relevant physics: waves interacting with a structure, wind interacting with a structure, and wind-wave interaction. The current work aims to address the first physics subset, wave-structure interaction, by validating multiphase numerical simulation against a wave flume experiment conducted at Oregon State University (Lomonaco, 2019).

2. METHODS

2.1. Experimental Dataset

The simulations aim to reproduce an experiment performed by Lomonaco et al. at Oregon State University (Lomonaco, 2019). Waves were simulated in an 87m long, 3.66 m wide and 4.57 m tall flume. The bathymetry, shown in Figure 1, includes an initial plateau with depth 2m, a 1:12 shoal, a second 21.96 m long plateau at 1.4m depth, and a dissipative beach at a 1:12 slope. Regular, irregular, and solitary wave experiments were performed both with and without a steel cylinder on the plateau. Wave gauges and acoustic doppler velocimeters (ADVs) measured water elevation and velocity profiles along the flume. The cylinder was instrumented with additional wave gauges and ADVs, as well as pressure gauges, load cells, accelerometers, and a high-speed video camera recording wave run-up. Experiments were run for roughly 60 wave periods.

The initial simulations presented in this abstract consider an Airy wave with no cylinder present in the domain. The Airy (Stokes I) wave is calibrated at Wave Gauge 1 (WG1) to have height 0.3m, period 3s, and initial water depth 2m. As validated shoaling is necessary for future work studying wind-wave interaction, this abstract presents comparisons of experimental and numerical results for mean and phase-averaged profiles of water elevation at multiple locations along the flume. In future work, loading on the cylinder will be compared using mean and wave-phase-averaged statistics. Phase-averaged profiles are produced by calculating signal phase using a Hilbert transform and averaging by phase bin (Hristov, 1998).

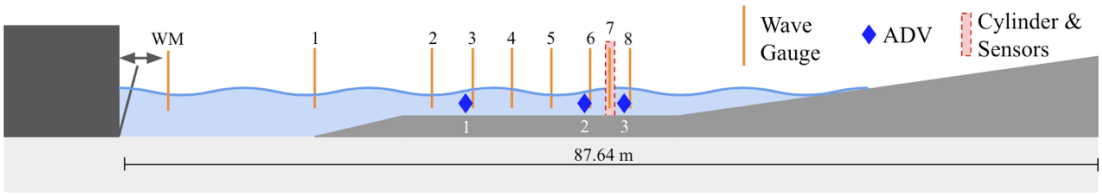

Figure 1. A schematic of the experimental wave flume set-up with removable steel cylinder.

2.2. Numerical Framework

OpenFOAM-v2112, an open-source finite volume solver, is used to perform multiphase simulations with the volume-of-fluid (VOF) method. Two interface capturing schemes, MULES and isoAdvector, have been explored, and the isoAdvector scheme was selected after proving more robust for the unstructured meshes needed to represent complex geometries.

Multiple turbulence modelling approaches, including Reynolds-averaged Navier-Stokes (RANS) and large-eddy simulations (LES), were examined. Recent literature has noted that overprediction of turbulence with traditional RANS models leads to unrealistic wave damping and proposed modified models such as the buoyancy-modified stabilized RANS k-omega SST to address this issue (Larsen, 2018). However, these models operate by imposing artificial limits on the turbulent eddy viscosity, which may result in errors in the air phase where higher turbulence is naturally expected. LES models are able to adapt between regions of high turbulence and nearly potential flow beneath surface waves to appropriately propagate waves down a flume, with a similar computational cost. Hence, this abstract presents the LES results, since LES with

the wall-adapting local eddy viscosity subgrid scale model was found to best adapt between potential flow regions beneath surface waves and turbulent regions elsewhere within the domain.

The numerical domain contains 90,000 cells in 2D and roughly 5 million cells in 3D. Discretization is performed using a Gauss linear second order-accurate scheme for spatial gradients and implicit Euler for time derivatives. The CFL is limited to 0.05 (Larsen, 2018), the adjustable time step varies between 1e-6 and 1e-3 seconds, and the simulation is run for 100 wave periods (300 seconds). The grid is refined along the air-water interface to 10 cells across the interface while maintaining an aspect ratio close to 1. The grid is also refined along the bottom to meet cell size requirements from the wall functions, which must adapt to a friction velocity that oscillates over the wave period. The mesh is carefully refined at the ramp where these two mesh quality requirements overlap.

The bottom and outlet are walls, and top of the flume is modelled as a Neumann boundary condition. In 3D simulations, the sides of the flume are additionally modelled as walls. Waves are generated at the inlet boundary condition using IHFOAM, which applies volume fraction and velocity profiles in cells along the boundary. In the experiment, the piston wavemaker applies an adjusted wave profile to produce the 'nominal' Airy wave at the calibration wave gauge, which in this experiment is Wave Gauge 1 (WG1). Initial results compare two versions of the wave-generating inlet boundary condition; the first applies the nominal Airy wave, and the second applies the wave observed at the experiment's WaveMaker Wave Gauge (WM WG).

3. RESULTS

Figure 2 presents an instantaneous snapshot of 2D numerical simulations of the Airy wave under consideration. The snapshot includes volume fraction, horizontal velocity, and vertical velocity in both air and water phases as the wave shoals and then breaks on the flume's dissipative beach.

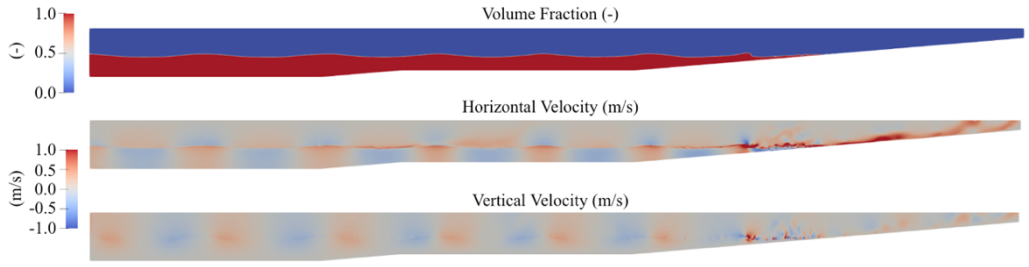

Figure 2. A snapshot of simulation results including instantaneous volume fraction, horizontal and vertical velocity fields from an initial 2D numerical simulation output (without cylinder). Low volume fraction (blue) corresponds to air phase, and high volume fraction (red) represents the water phase.

In Figure 3, initial mean and phase-averaged water elevation profiles for the Airy wave with height 30cm, period 3sec, and depth 2m are presented, with the two wave generation boundary conditions compared against experimental results. When applying the nominal wave at the inlet boundary condition, the mean wave height at all wave gauges has less than 5% error from the experiment, and the phase-averaged wave elevation profile at WG1 matches the experiment with less than 2% error throughout the wave period. However, after shoaling, this boundary condition results in a phase-averaged crest height underpredicted by as much as 20% in the nonlinear wave

profile observed at the cylinder location (WG7). The second inlet boundary condition, which applies the wave profile observed at the experiment's wavemaker, improves nonlinearity after shoaling but still shows significant underprediction of the phase-averaged trough height and produces large errors in mean wave height throughout the flume.

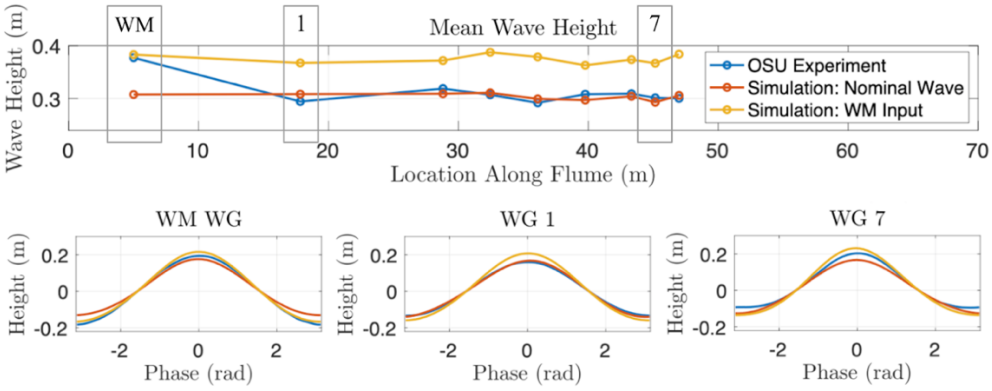

Figure 3. Mean and phase-averaged wave elevation statistics are compared for wave gauges at the wavemaker (WM WG), at the nominal wave calibration point (WG 1), and at location of the cylinder installation (WG 7). The cylinder was not present for this experiment.

In ongoing work, we are investigating improvements to the shoaling prediction by examining best practices to calibrate the input wave profiles and to match the reflection absorption action of the experimental piston wavemaker in the simulations. Subsequently, we will consider loading on the cylinder, comparing pressure distributions, total force, and wave run-up measurements between experiment and simulations. Additionally, mean wind profiles, spectra, and turbulent statistics will be examined in the air phase, and influential model parameters will be identified. Future work will further extend the validation of the current framework for wind-wave and wind-structure interaction.

ACKNOWLEDGEMENTS

This work is supported by a Gabilan Stanford Graduate Fellowship and a Stanford Enhancing Diversity in Graduate Education Doctoral Fellowship. CFD simulations were performed on the Sherlock computing cluster, with resources and support provided by the Stanford Research Computing Center.

REFERENCES

Buckley, M. P., and Veron, F., 2016. Structure of the Airflow above Surface Waves. Journal of Physical Oceanography 46, 5, 1377-1397.

Higuera, P., Lara, J. L., and Losada, I. J., 2013. Realistic wave generation and active wave absorption for Navier–Stokes models: Application to OpenFOAM®. Coastal Engineering 71, 102-118.

Hristov, T., Friehe, C., and Miller, S., 1998. Wave-coherent fields in air flow over ocean waves: identification of cooperative behavior buried in turbulence. Phys. Rev. Lett. 81, 5245–48.

Larsen, B. E. and Fuhrman, D. R., 2018. On the over-production of turbulence beneath surface waves in Reynolds-averaged Navier–Stokes models. Journal of Fluid Mechanics 853, 419–460.

Lomonaco, P., et. al., 2019. 29th International Ocean and Polar Engineering Conference "Physical Model Testing of Wave Impact Forces on Fixed Foundations of Offshore Wind Turbines." 16-19 June 2019. Honolulu, HI, USA.

OpenFOAM®, n.d. OpenFOAM® [WWW Document]. URL https://www.openfoam.com/ (accessed 1.26.23).

Roenby, J., Bredmose, H. and Jasak, H., 2016. A computational method for sharp interface advection. Royal Society open science, 3(11), 160405.